

STRUCTURE DESIGN AND LEVELLING CONTROL SYSTEM DEVELOPMENT FOR SELF-PROPELLED SPRAYER BOOM

自走式喷雾机喷杆结构与仿形调平控制系统开发

Zhenyu ZHANG¹, Jiayu CAO¹, Peijie GUO¹, MiaoYun WANG², Yu CHEN^{*1}

¹ College of Mechanical and Electronic Engineering, Northwest A&F University, Yangling, 712100, China;

² College of Intelligent Manufacturing, Shaanxi Institute of Mechatronic Technology, Baoji, 721001, China;

Tel: +86 17795759790; E-mail: jdx73@nwfau.edu.cn

DOI: <https://doi.org/10.35633/inmateh-75-17>

Keywords: Self-propelled sprayer, spray boom, levelling control system, adjustment threshold, ultrasonic distance sensor, performance experiment

ABSTRACT

To address the issues of poor boom stability and inconsistent spray quality due to harsh field conditions and varying boom height relative to the target, a five-section planar truss boom capable of height adjustment, overall tilt adjustment, and unilateral tilt adjustment was designed. A contour levelling control system for the boom was developed based on the STM32F103 platform. The levelling system uses ultrasonic distance sensors to detect the distance between the boom's ends and the target in real-time. The limit average filtering method is employed to eliminate sudden signal interference and process feedback data. The control system then drives electric actuators to adjust the boom's posture in real-time. Field and spray tests were conducted using a small electric self-propelled sprayer as the test platform. The results indicate that the best levelling performance was achieved with overall height adjustment, overall tilt adjustment, and unilateral tilt adjustment thresholds set to 30 mm, 30 mm, and 40 mm, respectively. The field spray tests showed minimal relative errors in droplet deposition coverage and density on both sides. The coefficient of variation CV of deposition along the boom direction was less than 15%, ensuring good spray distribution uniformity. These findings provide valuable references for the design and optimization of sprayer booms.

摘要

本文设计了一种可实现高度调节、整体倾斜调节、单侧倾斜调节功能的平面五段式桁架喷杆。基于STM32F103平台设计了喷杆仿形调平控制系统，调平系统采用超声波测距传感器实时检测喷杆两侧末端与目标物之间距离，利用限幅平均滤波法以排除突变信号的干扰并对反馈数据进行计算处理，控制系统驱动各机构电动推杆伸缩对喷杆姿态进行实时调整。以小型电动自走式喷雾机为试验平台，分别进行了场地试验及田间喷雾试验，场地试验结果表明当设定整体高度调节阈值为30mm、整体倾斜调节阈值为30mm、单侧倾斜调节阈值为40mm时调平效果最佳，田间喷雾试验结果表明两侧雾滴沉积覆盖率及沉积密度相对误差较小，沿喷杆向上的沉积量变异系数CV小于15%，可以保证较好的喷雾分布均匀性，研究成果为喷雾机喷杆的设计与优化提供了参考。

INTRODUCTION

Self-propelled boom sprayers are widely used in field pest and disease control due to their high operational efficiency and excellent spray quality (Dou et al., 2021; Baltazar et al., 2021; Lin et al., 2022). However, harsh field conditions often cause the sprayer to pitch, roll, and yaw, leading to boom imbalance relative to the ground, and in severe cases, the boom ends may even touch the ground (Ali et al., 2023; Li et al., 2023; Lipiński et al., 2022). Furthermore, to ensure spray quality, the boom should maintain an optimal and nearly parallel distance to the crop canopy. Therefore, the boom height must automatically adjust in real-time according to changes in crop canopy height and terrain to ensure uniform spray distribution and operational safety (Dou et al., 2021; Dou et al., 2021; Bayat et al., 2018). To this end, researchers both domestically and internationally have conducted studies on boom levelling control. Llica et al. (2018) studied boom height measurement methods and developed an automatic height adjustment control algorithm to maintain a constant

¹ Yu CHEN, Prof. Ph.D. Eng; Zhenyu ZhANG, M.R. Stud. Eng; Jiayu CAO, M.R. Stud. Eng; Peijie GUO, M.R. Stud. Eng;

² MiaoYun WANG, M.S. assistant, Eng.

distance between the nozzle tip and the target area (soil or canopy), enhancing the sprayer's application efficiency. Okamoto et al. integrated multiple sensors to detect the boom's posture, providing precise detection methods for the boom adjustment system (Okamoto et al., 2015). An Jiahao et al., (2022), designed a boom levelling mechanism based on the pendulum suspension principle, allowing the boom to swing left and right between -20° and 20° relative to the vehicle body. Based on this principle, they developed a boom levelling control system. Sun Xing et al., (2020), used a weighted average algorithm to integrate data from inclination sensors and ultrasonic sensors, and based on this, designed an expert-controlled boom height adjustment system. Zhang Meng et al., (2019), designed an automatic boom levelling control system using inclination sensors based on MEMS inertial navigation technology to achieve real-time boom posture adjustments.

This study focuses on the boom of a small electric sprayer, aiming to enhance boom operational stability and spray uniformity by designing a boom structure capable of ground contour following. Based on its working principle, ultrasonic sensors are used to detect the distance between the boom and the spraying target. The limit average filtering method is employed to eliminate sudden signal changes, and the boom contour levelling control is achieved by controlling the forward and reverse rotation and extension of electric actuators in each mechanism.

MATERIALS AND METHODS

Overall structure of the boom

The boom contour levelling system is designed based on our team's independently developed small self-propelled electric sprayer, with the overall boom structure shown in Fig. 1. The boom uses a five-section planar truss structure (left small boom, left large boom, middle boom, right small boom, right large boom), the small booms are connected to the large booms via small boom folding mechanisms, and the large booms are connected to the middle boom via unilateral tilt mechanisms and large boom folding mechanisms, the middle boom is connected to the boom mounting frame through an overall tilt mechanism, while the boom mounting frame is connected to a parallelogram lifting mechanism for height adjustment. The parallelogram lifting mechanism is connected to the chassis to secure the entire boom.

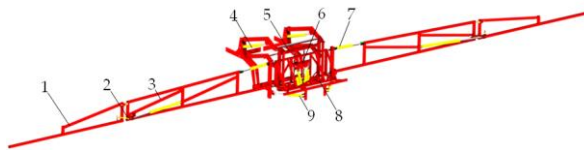


Fig. 1 - High clearance self-propelled sprayer test platform

1 – Small boom; 2 – Small boom folding mechanism; 3 – Large boom; 4 – Parallelogram lifting mechanism; 5 – Boom mounting frame; 6 – Overall tilt mechanism; 7 – Unilateral tilt mechanism; 8 – Middle boom; 9 – Large boom folding mechanism

Design of key mechanisms

(1) Design of the parallelogram lifting mechanism

The parallelogram lifting mechanism primarily consists of a boom mounting frame, upper link, lower link, boom bracket, and height-adjusting push rod, as shown in Fig. 2. The boom bracket is bolted to the sprayer chassis through pre-set bolt holes, securing the entire parallelogram lifting mechanism to the sprayer frame. The boom bracket and boom mounting frame are connected via the upper and lower links, which are of equal length and remain parallel during height adjustment. This forms a double parallelogram linkage. The double link structure enhances structural strength and prevents deformation during height adjustment.

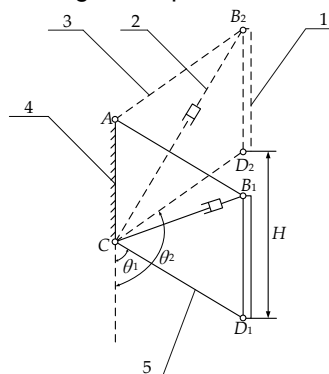


Fig. 2 - Operating principle of the parallelogram lifting mechanism

1 – Boom mounting frame; 2 – Height-adjusting push rod; 3 – Upper link; 4 – Boom bracket; 5 – Lower link

In Fig. 2, quadrilateral AB1CD1 represents the lowest position of the parallelogram lifting mechanism, and AB2CD2 represents the highest position. l_{AB} is the length of the upper link, l_{CD} is the length of the lower link, l_{AC} is the length of the fixed end of the boom bracket, θ_1 and θ_2 are the angles between the lower link and the vertical direction at the extreme positions of the boom. H denotes the maximum height adjustment distance of the boom.

As shown in Fig. 2, the maximum range of boom height adjustment is:

$$H = |l_{CD} (\cos \theta_2 - \cos \theta_1)| \tag{1}$$

The minimum length of the height-adjusting electric push rod is:

$$L_{\min} = \sqrt{l_{AB}^2 + l_{AC}^2 - 2l_{AB}l_{AC} \cos \theta_1} \tag{2}$$

The maximum length of the height-adjusting electric push rod is:

$$L_{\max} = \sqrt{l_{AB}^2 + l_{AC}^2 - 2l_{AB}l_{AC} \cos \theta_2} \tag{3}$$

If h_1 is the minimum distance from the fixed end of the boom bracket to the ground, and h_2 is the distance from the lower link hinge point of the parallelogram lifting mechanism to the bottom of the boom, then the minimum adjustable height of the boom is,

$$h = h_1 - l_{AB} \cos \theta_1 - h_2 \tag{4}$$

(2) Design of the overall inclination mechanism

The working principle of the overall inclination mechanism is shown in Fig. 3. Figures 3(a), (b), and (c) represent the left limit, horizontal, and right limit states of the spray boom. When the overall tilt angle range is set to -5° to 5° , the angles between the tilt link and the overall tilt push boom at their left and right limit positions are:

$$\theta_L = \arcsin \frac{l_a}{l_b \sin \delta} + 5^\circ, \quad \theta_R = \arcsin \frac{l_a}{l_b \sin \delta} - 5^\circ \tag{5}$$

The length of the overall tilt push boom is:

$$l_a^2 + (l - l_L)^2 - 2l_a(l - l_L) \cos \theta_L = l_b^2, \quad l_a^2 + (l + l_R)^2 - 2l_a(l + l_R) \cos \theta_R = l_b^2 \tag{6}$$

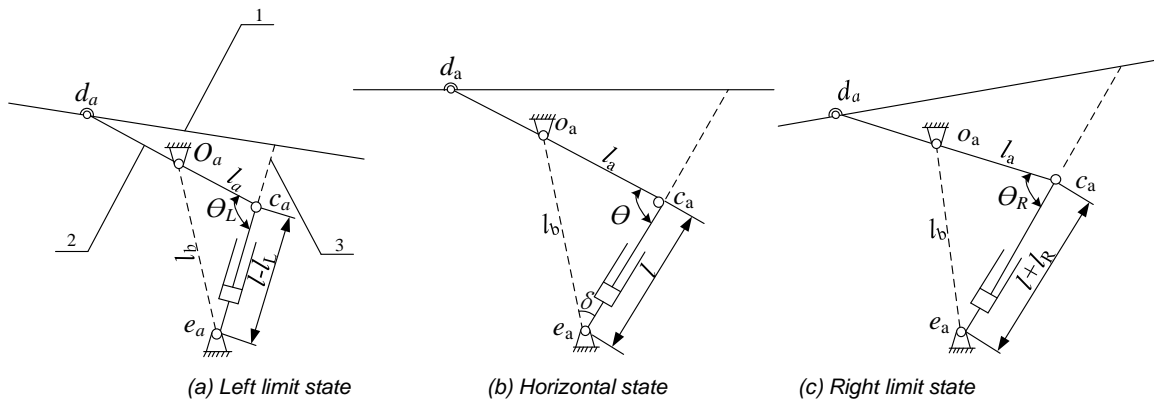


Fig. 3 - Working principle of the overall inclination mechanism
 1 – Central spray boom; 2 – Inclined link rod; 3 – Integrated inclined push rod

As shown in Fig. 4, the three-dimensional model of the integrated tilting mechanism allows relative rotation among the inclined link rod, the welded inclined plate, and the central spray boom. Additionally, the relative rotation is possible between the inclined link rod and the fixed column. By controlling the extension and retraction of the electric push rod, the overall inclination of the spray boom can be achieved. When the small-range height adjustment push rod remains stationary, shortening the integrated inclined push rod causes the right end of the inclined link rod to rotate around its center, transferring thrust to the fixed column at the left end. Since the fixed column is welded to the central spray boom, this results in a clockwise rotation and inclination of the spray boom. Conversely, when the integrated inclined push rod extends, the spray boom rotates counterclockwise. When both the small-range height adjustment push rod and the integrated inclined push rod extend or retract simultaneously at the same speed, the welded inclined plate, inclined link rod, central spray boom, and guide plate move together along the guide tube, achieving small-range height adjustment of the spray boom.

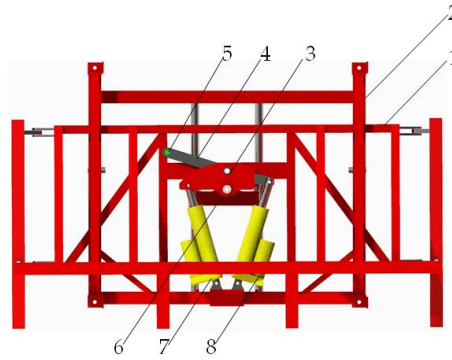


Fig. 4 - Overall inclination mechanism

1 – Central spray boom; 2 – Spray boom mounting bracket; 3 – Welded inclined plate; 4 – Inclined link rod; 5 – Fixed column; 6 – Guide plate; 7 – Small-range height adjustment push rod; 8 – Integrated inclined push rod

(3) Design of the unilateral tilting mechanism

Taking the right spray boom as an example, the working principle of the unilateral tilting mechanism is shown in Fig.5. One end of the unilateral tilting push rod is hinged to the fixed rod of the large arm spray boom, while the other end is hinged to the large arm spray boom itself. The unilateral tilting rotating block is connected to the pin shaft below the fixed rod of the large arm spray boom, the large arm spray boom can rotate at a certain angle around the fixed rod through the rotating block. When the unilateral tilting push rod contracts, it drives the large arm spray boom to rotate clockwise, when the unilateral tilting push rod extends, it drives the large arm spray boom to rotate counter clockwise, thereby achieving the tilting adjustment of the unilateral spray boom.

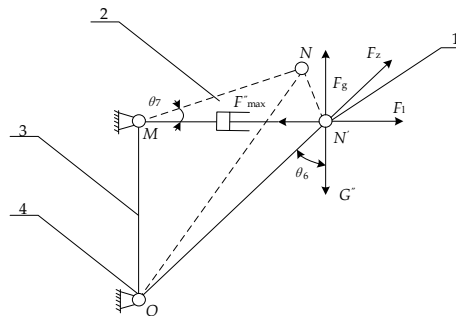


Fig. 5 - Working principle of the unilateral inclination mechanism

1 – Large arm spray boom; 2 – Unilateral inclination push rod; 3 – Large arm spray boom fixing rod; 4 – Unilateral inclination rotating block

The length of the unilateral inclination push rod at the extreme rotation position of the spray boom is,

$$l_{MN'} = l_{MN} \cos \theta_7 \tag{7}$$

The support force provided by the pin to the main arm spray boom is,

$$F_z = F_g / \cos \theta_6 \tag{8}$$

$$F_g = G'' \tag{9}$$

The maximum thrust required by the single-sided inclined push rod is,

$$F_{max}^* = F_1 = F_z \cos(90^\circ - \theta_6) \tag{10}$$

Design of the boom profiling and levelling system

(1) Working principle of the system

Currently, boom levelling systems primarily use distance sensors to detect boom height or tilt sensors to measure boom inclination (Li et al., 2020; Wang et al., 2019; Fu et al., 2020; Zürey et al., 2020; Burgers et al., 2021). Tilt sensors can measure the entire boom's tilt angle in dynamic environments and are widely used in small drones, intelligent agricultural equipment, and automobiles (Li et al., 2023; Shi et al., 2020; Yan et al., 2021). However, the boom designed in this paper is divided into five sections during profiling and levelling, allowing for separate control of the overall boom and the two sides. The use of tilt sensors alone cannot meet control requirements, so ultrasonic distance sensors are selected for real-time boom height detection.

The working principle of the boom contour levelling system is shown in Fig. 6. An ultrasonic distance sensor is installed at the end of each small arm on both sides of the boom, measuring the height of the side

booms and the overall boom above the ground. The controller processes the sensor feedback data to drive height adjustment, overall tilt, and single-side tilt electric push rods to adjust the height of each boom section, ensuring precise levelling for various terrains. To avoid repetitive adjustments near the target height during levelling, a height adjustment threshold is set. When the real-time collected boom height falls within the threshold range, the system automatically stops the levelling action.

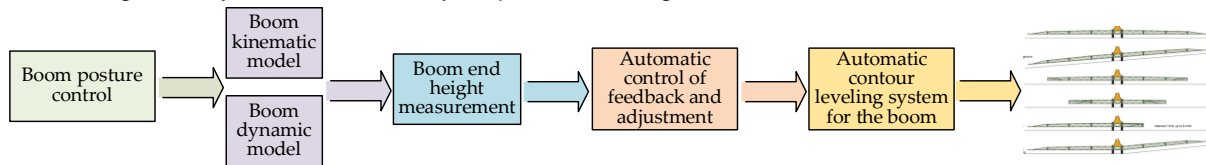


Fig. 6 - The working principle of the boom contour levelling system

The boom contour levelling control system is designed with an STM32 micro-controller as its core, with its hardware structure shown in Fig. 7. The system uses two ultrasonic distance sensors to accurately measure the ground clearance on both sides of the boom, and the detected data is input into the microprocessor for filtering and evaluation. Based on the levelling requirements, the microprocessor generates corresponding control signals to operate the H-bridge module, driving the appropriate electric actuators to adjust the boom's height or angle, thus providing real-time posture adjustments. The distance sensors are HY200P4C ultrasonic sensors with built-in temperature compensation, having a detection range of 100-2000 mm. The communication protocol used is RS485, which supports high-speed and long-distance data transmission, making it suitable for wide boom sprayers. The response time is 40 ms, with a repeat accuracy of 0.3%. The data conversion module is the GN-15 RS485-TTL module, which supports a wide voltage range (3.0-33V) and baud rates of 110-460800 BPS. The motor drive module uses the GZ-PMDC-120A7T H-bridge L298 logic speed controller, with an input voltage of 12-27V and a rated output current of 7A. Fast recovery diodes are used to prevent the control section from being damaged by large counter-electromotive forces during motor startup. The microprocessor selected is the STM32F103ZET6 based on the Cortex-M3 core, featuring 112 I/O ports, 5 UART communication ports, and 1 CAN communication port.

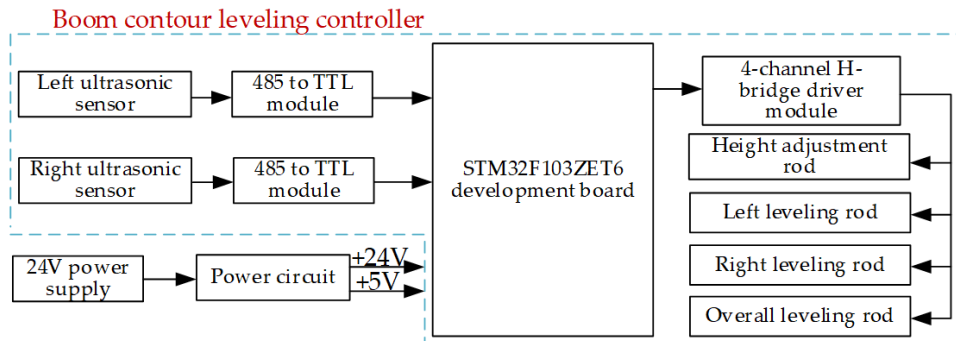


Fig. 7 - The hardware structure for boom contour levelling

(2) Information acquisition and processing of ultrasonic distance sensors

When the sprayer operates in the field, ultrasonic distance sensors are used to send measurement signals to the crop canopy. However, the spacing between crops may cause the signals to pass through gaps and reach the ground, resulting in abrupt changes in measurement values and leading to erroneous judgments by the control system. To ensure the accuracy of height information, it is necessary to apply filtering to exclude interference from sudden signal changes during data collection. After comparing various filtering techniques, the amplitude-limited averaging filter method was selected for processing the sensor signals. This method effectively eliminates deviations caused by occasional pulse interference and provides good signal smoothing (Li et al., 2022). The filtering principle is as follows: based on the plant height at different application stages, the maximum allowable deviation value A between two successive samples is determined. If the difference between the current sample value and the previous one is less than or equal to A , the current sample value is accepted; otherwise, it is discarded, and the previous value is used instead.

The filtering algorithm, shown in Equation (11), averages 20 samples that meet the criteria. If the deviation exceeds the pressed height range, the output signal drives the electric actuator to adjust the boom position.

$$y'(k) = \begin{cases} y(k), & |y(k) - y(k-1)| \leq A \\ y(k-1), & |y(k) - y(k-1)| > A \end{cases} \quad (11)$$

In the equation, $y(k)$ represents the k -th sample value, $y(k-1)$ represents the $k-1$ -th sample value, A is the maximum allowable deviation between two successive sample values, and $y'(k)$ denotes the signal value after the k -th filtering process.

(3) Control logic of the contour levelling system

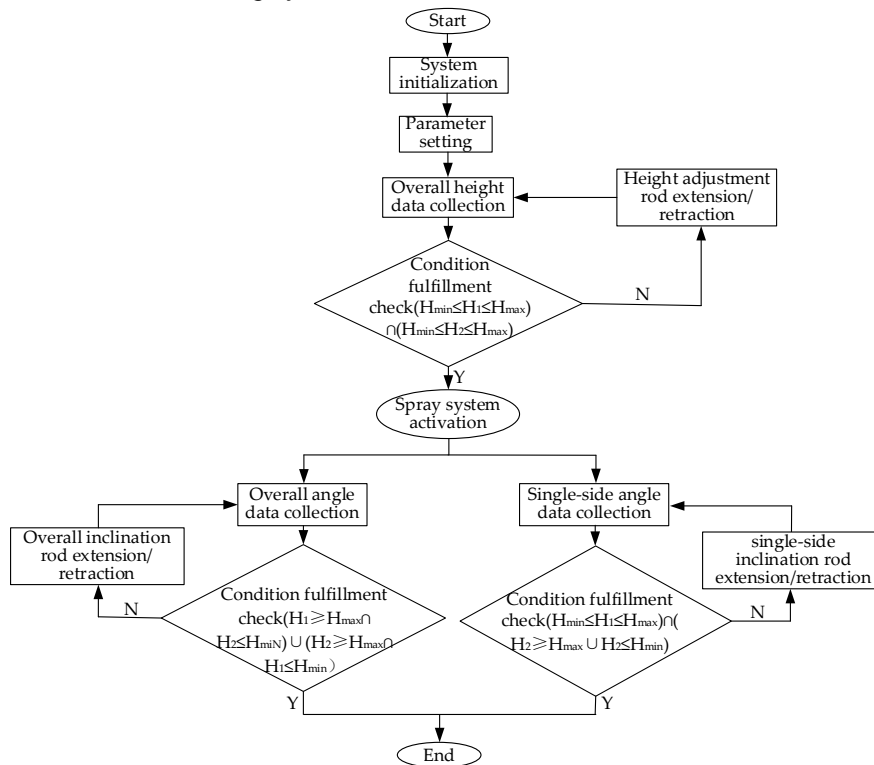


Fig. 8 - The terrain following levelling process

When the sprayer enters the field, the boom is fully extended, operator activates the ground contour levelling control system, upon entering the main program, the overall height of the crop canopy is first adjusted. If the heights on both sides do not fall within the preset range, the height adjustment rod drives the parallelogram lift mechanism to adjust the overall height of the boom. When both sides meet the preset height requirements, the spraying system is activated, and the sprayer enters the boom angle adjustment program. Angle adjustment includes both overall and single-side adjustments. If one side is below the minimum preset height and the other side is above the maximum preset height, an overall angle adjustment is performed, with the inclination rod adjusting the overall boom angle. If one side meets the preset height range while the other does not, a single-side angle adjustment is performed, with the inclination rod adjusting the angle of the single side. After adjustment, the system returns to the angle adjustment program for continuous monitoring. After spraying is completed, the ground contour levelling control system is turned off, the booms are adjusted to their initial extended state, and the booms are folded for transport.

(4) Experimental methods and procedures

The terrain in the field during the operation of the sprayer is complex and variable. To simulate the imbalance of the spray boom caused by field undulations, a stepped test site and a single-sided inclined surface were designed. To simulate the wheat plant height at different growth stages, the optimal preset distance between the spray boom and the crop canopy was adjusted. These three sets of experiments were used to verify the effectiveness of the spray boom ground contour levelling control system. After comparing the data from each experiment, the optimal threshold parameters for the control system were selected. To verify the designed spray boom's performance, spray tests were conducted in a wheat field. The spray boom ground contour levelling test methods and procedures are shown in Fig. 9.

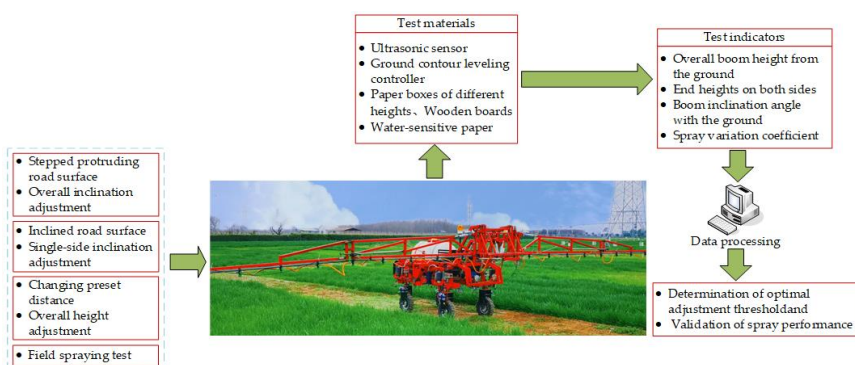


Fig. 9 - Spray boom ground contour levelling test methods and procedures

Experimental methods and condition settings

(1) Spray boom overall height adjustment experiment

During the wheat growth cycle, plant height changes continuously. If the spray boom height is not adjusted, excessive spray overlap can lead to over-spraying or missed areas. The overall ground clearance of the spray boom can be adjusted using a parallel four-bar lifting mechanism. However, due to the difficulty of altering wheat plant height, the performance of spray boom height adjustment was validated by changing the preset height of the spray boom relative to the wheat canopy. Before the test, the spray boom was fully extended and its initial ground clearance was adjusted. Controller parameters were modified to set the target height of the spray boom above the crop canopy at 400, 500, and 600 mm, with height adjustment thresholds set at 20, 30, 40, and 50 mm. After setting these parameters, the sprayer was driven at a constant speed in a straight line, and the ground contouring control system was activated. Once the spray boom height stabilized, the control system was turned off and the overall height of the spray boom was recorded.

(2) Stepwise field experiment

During field operations, undulations in the ground surface prevent the boom from maintaining a nearly parallel state relative to the application target. To simulate the inclination of the boom relative to the target during sprayer operation, a stepwise test surface was designed, as shown in Fig. 10.

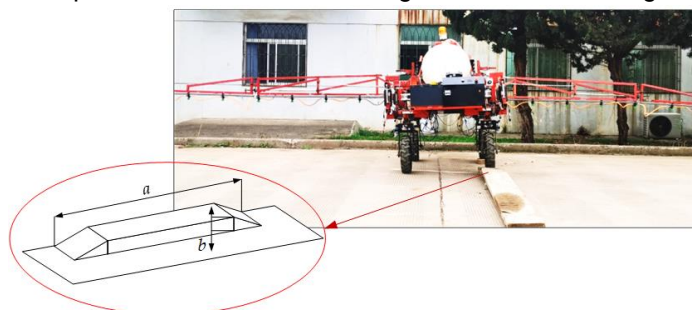


Fig. 10 - Stepwise field experiment

The designed boom has a maximum spray width of 9000 mm, and the sprayer's wheel track is 1200 mm. If the height b of the stepwise surface is set to 50 and 100 mm, and the length a is set to 5000 mm, the maximum tilt angle of the boom relative to the ground can reach 4.8° , causing a maximum displacement of 400 mm at the boom's end. To prevent collisions between the boom and the ground, the boom height was set to 700 mm, and adjustment thresholds were set to 20, 30, 40, and 50 mm. After stabilizing the boom height using the ground contour levelling system, the sprayer was driven over the stepwise surface at a constant speed of 8 km/h for four adjustment thresholds. After the front and rear right-side tires completely entered the highest point and the boom height stabilized, the control system was turned off. The heights of the boom ends on both sides and the tilt angle of the boom relative to the ground were recorded.

(3) Single-side inclination adjustment experiment

During field operations, the sprayer boom may encounter asymmetrical terrain within its coverage area. As shown in Figure 11(a), after overall tilt levelling, one side of the boom meets the spraying requirements, but the other side still fails to remain parallel to the application target. However, single-side tilt levelling can independently control the boom's posture on each side, as illustrated in Figure 11(b), enabling the boom to follow asymmetric terrain changes and maintain the optimal spraying height.

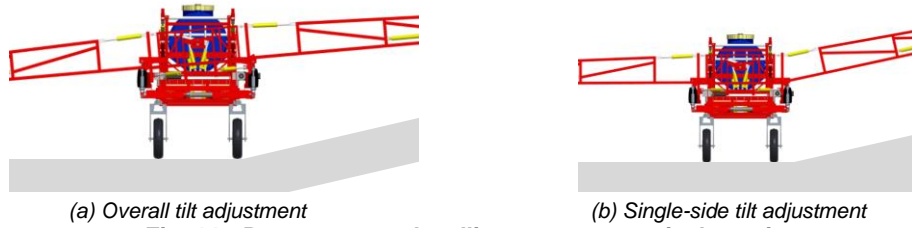


Fig. 11 - Boom contour levelling on asymmetrical terrain

The single-sided tilt adjustment test setup is shown in Fig.12, where a 10° tilted road surface was constructed beneath the right spray bar using wooden boards and cloth.



Fig. 12 - Single-sided inclination adjustment test

To prevent the spray bar from scraping against the tilted road surface, the height of the spray bar was set to 900 mm before the experiment. The adjustment thresholds were set to 20, 30, 40, and 50 mm, respectively. After stabilizing the height of the spray bar using the ground simulation levelling system, the sprayer was driven at a constant speed of 8 km/h over the tilted road surface at each of the four adjustment thresholds. Forward movement was stopped when the ultrasonic sensor detected the tilted road surface. After the spray bar height stabilized, the control system was shut down, and the angle of the right spray bar was recorded.

(4) Field spraying experiment

Water-sensitive papers were fixed to wheat plants at 25 cm intervals along the transverse direction of the spray bar to collect droplets (excluding the central 2 m of the road where the sprayer passes without wheat crops, totaling 24 water-sensitive papers). The spraying system was activated in advance to ensure that each nozzle reached the rated pressure when passing over the water-sensitive paper strip. The sprayer moved through the wheat field at a constant speed of 8 km/h. The power was turned off after the rear spray bar completely passed the water-sensitive paper strip. Once the water-sensitive papers dried naturally, they were collected into sealed bags (Liu et al., 2022). The droplet information was analyzed using the software ImagePy-master on the scanned water-sensitive papers. The experimental process is shown in Fig. 13.



Fig. 13 - Field spray test

RESULTS

The results of spray boom overall height adjustment experiment

The test results of spray boom overall height adjustment experiment are shown in Table 1.

Table 1

Results of the spray boom overall height adjustment test /mm

Target height	Adjustment threshold	Final stable height	Target height	Adjustment threshold	Final stable height	Target height	Adjustment threshold	Final stable height
/400	50	438	/500	50	531	/600	50	640
	40	420		40	517		40	626
	30	404		30	509		30	614
	20	instability		20	instability		20	instability

As shown in Table 1, when the height adjustment threshold is set between 30-50 mm, the boom profiling levelling control system stabilizes the boom height near the target value. As the adjustment threshold decreases, the overall boom height gradually approaches the target spraying height. However, when the adjustment threshold is set to 20 mm, overshoot occurs, causing the height adjustment rod to extend and retract repeatedly, failing to maintain a stable height. This instability is primarily due to the delay in the control system's input and output. The height adjustment rod maintains its previous action until it receives the next adjustment signal, leading to overshoot. Therefore, the adjustment threshold should be set to 30 mm for overall boom height adjustment.

The results of stepwise field experiment

The results of stepwise field experiment are shown in Table 2.

Table 2

Results of the stepwise field experiment

Step height/mm	Adjustment threshold/mm	Left end height/mm	Right end height/mm	Boom inclination angle/°
50	50	742	664	0.5
	40	729	675	0.35
	30	710	688	0.15
	20	/	/	/
100	50	746	670	0.5
	40	721	683	0.25
	30	714	684	0.2
	20	/	/	/

As shown in Table 2, the boom ground contour levelling control system effectively reduces the boom inclination caused by step surfaces. With different adjustment thresholds, the boom's inclination angle relative to the ground decreases as the threshold decreases. When passing over a 100 mm step surface, the boom inclination angle can be reduced to approximately 0.2°. However, with an adjustment threshold of 20 mm, an overshoot phenomenon occurs, causing the overall tilt push rod to repeatedly extend and retract, making it difficult for the boom to stabilize. The primary factor is the latency in the control system's input-output response, causing the overall tilt adjustment rod to maintain the previous adjustment action until the next signal is received, leading to overshoot. Therefore, the adjustment threshold should be set to 30 mm for the overall tilt adjustment of the boom.

The results of single-side inclination adjustment experiment

The results of Single-side inclination adjustment experiment are shown in Table 3.

Table 3

Results of the single-sided spray boom inclination adjustment test

Pavement inclination Angle /°	Adjustment threshold /mm	Right spray boom inclination angle /°	Relative error /%
10	50	9.2	8
	40	9.4	6
	30	9.6	4
	20	/	/

As shown in Table 3, the ground-following levelling control system for the spray bar effectively reduces single-sided spray bar inclination caused by uneven pavement. At different adjustment thresholds, the spray bar's inclination angle relative to the ground decreases as the adjustment threshold is reduced. When traversing a pavement with a 10° inclination angle, the single-sided spray bar can adjust to approximately 9.6°. However, when the adjustment threshold is set to 20 mm, the system experiences an overshoot phenomenon, causing repeated extensions and retractions of the single-sided tilt rod, making it difficult for the single-sided spray bar to achieve a stable state. To prevent instability caused by single-sided tilt adjustments after overall tilt adjustments, the single-sided tilt adjustment threshold is set to 40 mm.

The results of field spraying experiment

The results of the treatment of 24 water-sensitive papers were statistically analyzed. The papers on the left and right sides near the center of the road were labelled as Left 1 and Right 1, respectively. The results of the field spray test are shown in Tables 4 and 5.

Table 4

The results of the field spray test on the left side

Label	Droplet deposition coverage rate / %	Droplet deposition density / (Grain /cm ²)	Deposition amount / (μL/cm ²)
Left 1	33.44	179.33	1.26
Left 2	31.59	164.13	1.23
Left 3	35.63	172.64	1.21
Left 4	37.42	180.69	1.30
Left 5	38.71	175.38	1.25
Left 6	33.87	167.74	1.29
Left 7	39.64	181.42	1.35
Left 8	31.37	174.26	1.34
Left 9	35.79	183.97	1.27
Left 10	36.54	167.69	1.31
Left 11	34.46	171.56	1.26
Left 12	32.00	180.53	1.30

Table 5

The results of the field spray test on the right side

Label	Droplet deposition coverage rate / %	Droplet deposition density / (Grain /cm ²)	Deposition amount / (μL/cm ²)
Right 1	36.15	180.23	1.20
Right 2	34.20	168.19	1.26
Right 3	31.29	176.75	1.25
Right 4	35.49	184.46	1.31
Right 5	34.13	172.91	1.27
Right 6	34.85	183.10	1.29
Right 7	33.48	174.66	1.30
Right 8	35.69	178.43	1.29
Right 9	32.28	167.52	1.24
Right 10	37.51	171.67	1.32
Right 11	31.28	175.41	1.25
Right 12	30.66	180.42	1.34

Statistical processing was conducted on the spray test data from both sides of the nozzle to calculate the average fog droplet deposition coverage rate, the average fog droplet deposition density along the direction of the nozzle, and the coefficient of variation (CV) of deposition quantity. The results are shown in Table 6.

Table 6

Field spray test results			
Area	Average deposition coverage rate / %	Average deposition density / (Grain /cm ²)	Deposition variation coefficient (CV) / %
Left side	35.04%	174.90	3.1
Right side	33.92%	176.51	

As shown in Table 6, the average droplet deposition coverage rates on the left and right sides of the boom were 35.04% and 33.92%, respectively, and the average droplet deposition densities were 174.9 and 176.51 particles/cm², respectively. The relative errors in droplet deposition coverage and density between the two sides were minimal. The coefficient of variation (CV) of deposition along the boom direction was 3.1%, indicating that the sprayer exhibited good stability during field operations. The overall oscillation of the boom was minimal, ensuring uniform spray distribution.

CONCLUSIONS

(1) To ensure the optimal spraying height between the boom and the crop canopy, thereby improving spray quality, a five-section boom capable of ground contour following was designed. It includes a parallelogram lift mechanism, an overall tilt mechanism, and a single-side tilt mechanism. The boom height adjustment range is 360-1160 mm, the overall boom tilt angle range is -5° to 5°, and the single-side boom tilt angle range is 0° to 11°.

(2) A boom ground-following levelling control system was designed with the STM32F103ZET6 microprocessor at its core. This system employs ultrasonic distance sensors to detect the distance between the boom ends and the target objects in real-time. The microprocessor utilizes a limited amplitude averaging filter method to eliminate sudden signal interference and processes the feedback data to drive the electric actuators of each mechanism, thus adjusting the boom's position in real-time.

(3) A small electric self-propelled sprayer was used as the test platform to evaluate the performance of the boom ground-following levelling control system through various field tests. The results showed that the system performed best when the overall height adjustment threshold was set to 30 mm, the overall tilt adjustment threshold to 30 mm, and the single-side tilt adjustment threshold to 40 mm. The spray uniformity was assessed through field spray tests, which indicated that the relative error in droplet deposition coverage and density on both sides of the boom was minimal, and the coefficient of variation (CV) for deposition along the boom direction was less than 15%, ensuring good spray distribution uniformity.

ACKNOWLEDGEMENT

The research was funded by the Key R&D projects in Shaanxi Province (2024NC-YBXM-202, 2024NC-YBXM-244, 2023-YBNY-241).

REFERENCES

- [1] Ali B., Medet İ., Barış, Ö. Ö. (2023). Development and Assessment of A Novel Servo-controlled Spraying System for Real Time Adjustment of the Orientation Angle of the Nozzles of A Boom Sprayer. *Pest management science*, 79(11), 4439-4450. <https://doi.org/10.1002/ps.7644>.
- [2] An J. (2022). *Attitude Control Method and Test of Spray Rod of High Ground Clearance Pesticide Applicator*. Zibo: Shandong University of Technology.
- [3] Baltazar, A.R., Santos, F.N.D., Moreira, A. P., Valente, A., Cunha, J.B. (2021). Smarter Robotic Sprayer System for Precision Agriculture. *Electronics*, 10(17), 2061. <https://doi.org/10.3390/electronics10172061>.
- [4] Bayat, A., Itmec, M., Bolat, A. (2018). Modal Analysis of Field Sprayer Boom Design for Different Materials. *Scientific Papers-Seriesa-Agronomy*, LXI (6), 434-437.
- [5] Burgers, T. A., Gaard, J. D., Hyronimus, B. J. (2021). Comparison of Three Commercial Automatic Boom Height Systems for Agricultural Sprayers. *Applied Engineering in Agriculture*, 37(2), 287-298. <https://doi.org/10.13031/aea.14346>.
- [6] Dou, H., Zhai, C., Chen, L., Wang, X., Zou, W. (2021). Comparison of Orchard Target-Oriented Spraying Systems Using Photoelectric or Ultrasonic Sensors. *Agriculture*, 11(8), 753. <https://doi.org/10.3390/agriculture11080753>.

- [7] Dou, H., Zhai, C., Chen, L., Wang, S., Wang, X. (2021). Field Variation Characteristics of Sprayer Boom Height Using a Newly Designed Boom Height Detection System. *IEEE Access*, 9, 17148-17160. <https://doi.org/10.1109/access.2021.3053035>.
- [8] Dou, H., Wang, S., Zhai, C., Chen, L., Wang, X., Zhao, X. (2021). A LiDAR Sensor-Based Spray Boom Height Detection Method and the Corresponding Experimental Validation. *Sensors*, 21(6), 3390.
- [9] Fu, J., Chen, C., Zhao, R., Ren, L. (2020). Accurate Variable Control System for Boom Sprayer Based on Auxiliary Antidrift System. *Journal of Sensors*, 2020, 8037046. <https://doi.org/10.1155/2020/8037046>.
- [10] Lipiński, A. J., Lipiński, S., Burg, P., Sobotka, S. M. (2022). Influence of the Instability of the Field Crop Sprayer Boom on the Spraying Uniformity. *Journal of Agriculture and Food Research*, 10(9), 100432. <https://doi.org/10.1016/j.jafr.2022.100432>.
- [11] Li, J., Nie, Z., Chen, Y., Ge, D., Li, M. (2023). Development of Boom Posture Adjustment and Control System for Wide Spray Boom. *Agriculture*, 13(11), 2162. <https://doi.org/10.3390/agriculture13112162>.
- [12] Li, F., Bai, X., Su, Z., Tang, S., Wang, Z., Li, F., Yu, H. (2023). Development of a Control System for Double-Pendulum Active Spray Boom Suspension Based on PSO and Fuzzy PID. *Agriculture*, 13(9), 1660. <https://doi.org/10.3390/agriculture13091660>.
- [13] Li, F., Bai, X., Li, Y. (2020). A Crop Canopy Localization Method Based on Ultrasonic Ranging and Iterative Self-Organizing Data Analysis Technique Algorithm. *Sensors*, 20(3), 818.
- [14] Li, L., Hu, Z., Liu, Q., Yi, T., Han, P., Zhang, R., Pan, L. (2022). Effect of Flight Velocity on Droplet Deposition and Drift of Combined Pesticides Sprayed Using An Unmanned Aerial Vehicle Sprayer in A Peach Orchard. *Frontiers in Plant Science*, 13, 10129. <https://doi.org/10.3389/fpls.2022.981494>.
- [15] Liu, L., Liu, Y., He, X., Liu, W. (2022). Precision variable-rate spraying robot by using single 3D lidar in orchards. *Agronomy*, 12(10), 2509. <https://doi.org/10.3390/agronomy12102509>.
- [16] Li, C., Wu, J., Pan, X., Pan, X., Dou, H., Zhao, X., Gao, Y., Yang, S., Zhai, C. (2023). Design and Experiment of a Breakpoint Continuous Spraying System for Automatic-Guidance Boom Sprayers. *Agriculture*, 13(12), 2203. <https://doi.org/10.3390/agriculture13122203>.
- [17] Lin J., Xin W. (2022). Spray Deposition and Distribution on Rice as Affected by a Boom Sprayer with a Canopy-Opening Device. *Agriculture*, 13(1), 94. <https://doi.org/10.3390/agriculture13010094>.
- [18] Li, W., Yang, F., Mao, E., Shao, M., Sui, H., Du, Y. (2022). Design and verification of crab steering system for high clearance self-propelled sprayer. *Agriculture*, 12(11), 1893.
- [19] Llica, A., Boz, A. (2018). Design of a nozzle-height control system using a permanent magnet tubular linear synchronous motor. *Journal of Agricultural Sciences*, 24(3): 374-385. <https://doi.org/10.15832/ankutbd.456662>.
- [20] Okamoto, Y., Kameari, A., Fujiwara, K., Tsuburaya, T., Sato S. (2015). Fast Nonlinear Finite Element Analysis Using Newton-Raphson Method Implemented by Krylov Subspace Method with Relaxed Convergence Criterion. *COMPEL: The International Journal for Computation and Mathematics in Electrical and Electronic Engineering*, 34(5), 1537-1552.
- [21] Sun, X., Yang, X., Dong, X., Zhang, T., Yan, H., Wang, Z. (2020). Spray Boom Height Intelligent Adjustment System Based on Expert Control. *Transactions of the CSAM*, 32(S2), 275-282. <https://doi.org/10.3390/agriculture13091660>.
- [22] Shi, Y., Shu, X., Jiang, P., Hu, W., Lin, W., Dong, C. (2020). Design and Experimental Study on Automatic Levelling System of High Ground Gap Plant Protection System Chassis. *International Journal of Applied Systemic Studies*, 9(1), 11-25. <https://doi.org/10.1504/IJASS.2020.108656>.
- [23] Wang, G., Lan, Y., Yuan, H., Qi, H., Chen, P., Ouyang, F., Han, Y. (2019). Comparison of Spray Deposition, Control Efficacy on Wheat Aphids and Working Efficiency in the Wheat Field of the Unmanned Aerial Vehicle with Boom Sprayer and Two Conventional Knapsack Sprayers. *Applied Sciences*, 9(2), 218. <https://doi.org/10.3390/app9020218>.
- [24] Yan, J., Xue, X., Cui, L., Ding, S., Gu, W., Le, F. (2021). Analysis of Dynamic Behavior of Spray Boom Under Step Excitation. *Applied Sciences*, 11(21), 10129. <https://doi.org/10.3390/app112110129>.
- [25] Zhang, M., Hu, L., Ke, X., Tang, L., Meng, S., Du, P., Zhou, H., He, J. (2019). Design and Test of Automatic Levelling System for Spray Rod of Paddy Field Self-propelled Sprayer. *Agricultural Mechanization Research*, 41(10), 45-51.
- [26] Zürey, Z., Balci, S., Sabancı, K. (2020). Automatic Nozzle Control System with Ultrasonic Sensor for Orchard Sprayers. *European Journal of Technique*, 10(2), 264-273. <https://doi.org/10.36222/ejt.715015>.